ATLAS NOTE

ATL-PHYS-PUB-2014-016

October 21, 2014

Projections for measurements of Higgs boson signal strengths and coupling parameters with the ATLAS detector at the HL-LHC

The ATLAS Collaboration

Abstract

A study is presented on the ATLAS experimental prospects for measuring Higgs boson signal strengths, and determining couplings to individual fermions and bosons, using 14 TeV proton-proton collisions at the LHC with 300 fb^{-1} and at the HL-LHC with 3000 fb^{-1}. This document is released coincident with the 2014 ECFA HL-LHC workshop and contains updates since the 2013 workshop for the $H \to Z\gamma$ and $VH/ttH \to \gamma\gamma$ channels. In addition, the prospects for the $VH \to b\bar{b}$ channel have now been included in the combination of channels.

ATL-PHYS-PUB-2014-016
21 October 2014

1 Introduction

One of the main opportunities of an upgrade of the LHC to deliver high luminosity, the High-Luminosity LHC (HL-LHC), is to enable precise measurements of the Higgs boson properties. In the Standard Model (SM), all properties of the Higgs boson are defined once its mass is known. However, this model has many open questions such as the hierarchy problem and the nature of dark matter. Many alternative theories addressing these issues make different predictions for the properties of one or more Higgs bosons. Precise measurements in the Higgs sector are therefore a high priority in the future programme of particle physics. The ATLAS Collaboration presented a preliminary set of studies for the update of the European Strategy for Particle Physics [1] that are included in the Physics Briefing Book [2]; they are also included in the physics case in the ATLAS Phase-II upgrade Letter of Intent [3]. A more comprehensive study of the projected precision of measurements of the Higgs boson production cross section times branching ratios and Higgs boson couplings was presented at the ECFA HL-LHC workshop in 2013 [4].

The present LHC programme is expected to deliver a total integrated luminosity of about 300 fb^{-1} by the year 2022. The peak instantaneous luminosity will be in the range from 2 to 3$\times 10^{34}$ cm^{-2} s^{-1}. The luminosity will decrease from the peak value during a fill, so this sample is assumed to have a typical average number of pile-up events per bunch crossing, which is denoted here by μ_{pu}, of 50–60. The HL-LHC will deliver a total luminosity of about 3000 fb^{-1}, at a peak levelled luminosity of 5×10^{34} cm^{-2} s^{-1}, with a value of $\mu_{\text{pu}} = 140$.

The detector design for the high luminosity phase is not yet completely defined, and it will take years to adapt and optimise the event reconstruction software to the high-pile-up conditions. The goal is that the performance of the new detector in the harsh conditions of the high-luminosity phase will not be worse than the performance of the current detector with $\mu_{\text{pu}} \approx 20$. For the studies used in this note, the particle-level quantities were modified by applying efficiency and resolution ("smearing") functions to physics objects [5]. The assumptions regarding the performance are described in Ref. [6].

This note presents an update of the combination in Ref. [4]. The projections for some decay channels, $H \to Z\gamma$ [7] and $VH/ttH \to \gamma\gamma$ [8], have been revised. In addition, the prospects for the $VH \to b\bar{b}$ channel have been explored [9]. The measurements of the cross sections times branching ratio are expressed in terms of the ratio to the SM expectation, $\mu = \sigma/\sigma_{\text{SM}}$. The expected precision is given as the relative uncertainty in the signal strength, $\Delta\mu/\mu$. These measurements are then interpreted in terms of the Higgs boson couplings to elementary particles.

2 Input channels

This note presents the prospects for a combination of the $H \to \mu\mu$, $H \to \tau\tau$, $H \to ZZ$, $H \to WW$, and $H \to \gamma\gamma$ (0/1/2-jets categories) channels as presented in Ref. [4], the updates of $H \to Z\gamma$ and $VH/ttH \to \gamma\gamma$ categories presented in Refs. [7] and [8], respectively, and the recent study of $VH \to b\bar{b}$ prospects documented in Ref. [9]. The theory uncertainties in all channels have been updated as best as possible to reflect the current estimates [10–12]. The uncertainty on the Higgs boson branching ratios from the future precision on the Higgs mass measurement is not accounted for but is expected to be very small.

The HL-LHC projections for the $H \to \tau\tau$ channel are taken from Ref. [4], as the more detailed analysis in Ref. [13] covers only the $H \to \tau\tau \to \ell\nu\nu\,\tau_{\text{had.}}\nu$ decay mode assuming $\mu_{\text{pu}} = 140$ and a total luminosity of about 3000 fb^{-1}.

The precision on the signal strengths expected for each of these categories is presented in Fig. 1 and in Table 1. For the most precise categories, in the diboson final states, experimental uncertainties of ~5% are reachable with 3000 fb^{-1}. Table 2 illustrates the precision reachable for different production modes from combining different final states under the assumption of Higgs branching ratios as in the

SM. The cross section measurements of the dominant production mode, $gg \to H$, reach an ultimate experimental precision of ~4%, which is close to the limit given by the assumed luminosity uncertainty of 3%[1]. This will provide a stringent constraint on possible beyond-SM (BSM) contributions to the $gg \to H$ process, that is dominated in the SM by loop diagrams via top and bottom quarks. The rare $t\bar{t}H$ production cross-section should be measured with an ultimate precision of about ~10% and accordingly enable precise measurements of the top Yukawa-coupling (not including the $t\bar{t}H, H \to b\bar{b}$ channel in this projection). For illustration and in addition to the dominant $qq \to ZH$ process, the precision on the $gg \to ZH$ contribution is shown which becomes relevant at high $p_T(H)$ [14] in the $VH \to b\bar{b}$ channel. No special selection is made to enhance this production mode in the $H \to b\bar{b}$ analysis so the sensitivity is low. However, a dedicated analysis might allow to search for new physics in the $gg \to ZH$ loop process at the HL-LHC.

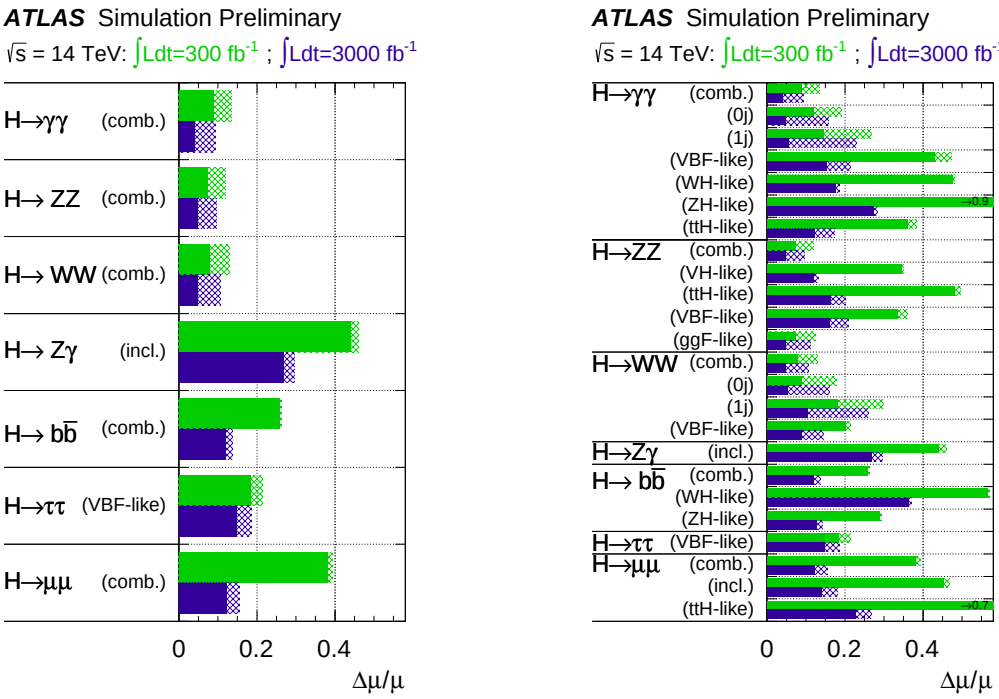

Figure 1: Relative uncertainty on the signal strength μ for all Higgs final states considered in this note in the different experimental categories used in the combination, assuming a SM Higgs boson with a mass of 125 GeV expected with 300 fb^{-1} and 3000 fb^{-1}of 14 TeV LHC data. The uncertainty pertains to the number of events passing the experimental selection, not to the particular Higgs boson process targeted. The hashed areas indicate the increase of the estimated error due to current theory systematic uncertainties. The abbreviation "(comb.)" indicates that the precision on μ is obtained from the combination of the measurements from the different experimental sub-categories for the same final state, while "(incl.)" indicates that the measurement from the inclusive analysis was used. The left side shows only the combined signal strength in the considered final states, while the right side also shows the signal strength in the main experimental sub-categories within each final state.

Additional information about the Higgs boson coupling properties can be gained through the search

[1] A luminosity uncertainty of 3% is assumed for both the 300 fb^{-1} and 3000 fb^{-1} scenarios, which has been agreed to by the ATLAS and CMS experiments for projections.

$\Delta\mu/\mu$	300 fb^{-1}		3000 fb^{-1}	
	All unc.	No theory unc.	All unc.	No theory unc.
$H \to \gamma\gamma$ (comb.)	0.13	0.09	0.09	0.04
(0j)	0.19	0.12	0.16	0.05
(1j)	0.27	0.14	0.23	0.05
(VBF-like)	0.47	0.43	0.22	0.15
(WH-like)	0.48	0.48	0.19	0.17
(ZH-like)	0.85	0.85	0.28	0.27
(ttH-like)	0.38	0.36	0.17	0.12
$H \to ZZ$ (comb.)	0.11	0.07	0.09	0.04
(VH-like)	0.35	0.34	0.13	0.12
(ttH-like)	0.49	0.48	0.20	0.16
(VBF-like)	0.36	0.33	0.21	0.16
(ggF-like)	0.12	0.07	0.11	0.04
$H \to WW$ (comb.)	0.13	0.08	0.11	0.05
(0j)	0.18	0.09	0.16	0.05
(1j)	0.30	0.18	0.26	0.10
(VBF-like)	0.21	0.20	0.15	0.09
$H \to Z\gamma$ (incl.)	0.46	0.44	0.30	0.27
$H \to b\bar{b}$ (comb.)	0.26	0.26	0.14	0.12
(WH-like)	0.57	0.56	0.37	0.36
(ZH-like)	0.29	0.29	0.14	0.13
$H \to \tau\tau$ (VBF-like)	0.21	0.18	0.19	0.15
$H \to \mu\mu$ (comb.)	0.39	0.38	0.16	0.12
(incl.)	0.47	0.45	0.18	0.14
(ttH-like)	0.74	0.72	0.27	0.23

Table 1: Relative uncertainty on the signal strength μ for the combination of Higgs analyses at 14 TeV, with 300 fb^{-1} (left) and 3000 fb^{-1} (right), assuming a SM Higgs boson with a mass of 125 GeV and assuming production cross sections as in the SM. For both 300 and 3000 fb^{-1} the first column shows the results including current theory systematic uncertainties, while the second column shows the uncertainties obtained using only the statistical and experimental systematic uncertainties. The abbreviation "(comb.)" indicates that the precision on μ is obtained from the combination of the measurements from the different experimental sub-categories for the same final state, while "(incl.)" indicates that the measurement from the inclusive analysis was used.

$\Delta\mu/\mu$	300 fb^{-1}		3000 fb^{-1}	
	All unc.	No theory unc.	All unc.	No theory unc.
$gg \to H$	0.12	0.06	0.11	0.04
VBF	0.18	0.15	0.15	0.09
WH	0.41	0.41	0.18	0.18
$qqZH$	0.80	0.79	0.28	0.27
$ggZH$	3.71	3.62	1.47	1.38
ttH	0.32	0.30	0.16	0.10

Table 2: Relative uncertainty on the signal strength μ for different production modes using the combination of Higgs final states at 14 TeV, with 300 fb^{-1} (left) and 3000 fb^{-1} (right), assuming a SM Higgs boson with a mass of 125 GeV and branching ratios as in the SM. For both 300 and 3000 fb^{-1} the first column shows the results including current theory systematic uncertainties, while the second column shows the uncertainties obtained using only the statistical and experimental systematic uncertainties.

for invisible Higgs decays [4, 15] and measurements of the off-shell Higgs production in WW and ZZ final states at invariant masses above the WW and ZZ on-shell production threshold [16–19]. Currently, no experimental projections of off-shell measurements at the HL-LHC exist. However, they should help to significantly enhance the knowledge about the total width [20].

3 Higgs boson couplings

The statistical treatment of the input channels used to extract information about the Higgs boson couplings is described in Refs. [4, 21–26].

The inclusive signal theory uncertainties for missing higher orders (QCD scale variations), PDF + α_S, and branching ratios (BR) are included as given in Refs. [10–12]. The correlations in the BR uncertainties for the different final states [10] are accounted for. For the (anti-)correlated uncertainty contributions for different jet multiplicities and Higgs p_T in the $gg \to H$ and $VH \to b\bar{b}$ processes, the same numbers as for the 7 and 8 TeV analysis are used [10, 27–29]. All common signal theory uncertainties are treated as being 100% correlated between all channels. For the luminosity an uncertainty of 3% is assumed. Other systematic uncertainties are considered to be analysis-specific and treated as uncorrelated between channels. In the following, two sets of results are presented: using the current theory uncertainties as summarized above or assuming no theory uncertainties, which is the expected experimental limit for a measurement. The true situation is therefore expected to lie between these extremes.

Following the approach recommended in Ref. [10], the leading-order tree-level motivated κ-framework is used to project the measurements of Higgs coupling scale factors at the HL-LHC. As this framework does not take into account higher order electroweak corrections beyond the SM, it is not deemed suitable for precision measurements. Instead an effective field theory (EFT) approach is currently seen as the most promising way for future Higgs precision measurements, as it allows to consistently calculate higher order corrections and also includes CP-odd couplings in a natural extension. Unfortunately such an EFT machinery is not available yet. However, the main degrees of freedom which are mainly constrained from Higgs measurements in such an EFT will be similar to the degrees of freedom present in the leading-order κ-framework, so the precision projections presented here for the HL-LHC should stay approximately valid.

3.1 Coupling fit framework

The measurements of coupling scale factors are implemented using a leading-order tree-level motivated framework [10]. This framework is based on the following assumptions:

- The signals observed in the different search channels originate from a single resonance. A mass of 125 GeV is assumed here.
- The width of the Higgs boson is narrow, justifying the use of the zero-width approximation. Hence the predicted rate for a given channel can be decomposed in the following way:

$$\sigma \cdot B\,(i \to H \to f) = \frac{\sigma_i \cdot \Gamma_f}{\Gamma_H} \tag{1}$$

  where σ_i is the production cross section through the initial state i, B and Γ_f are the branching ratio and partial decay width into the final state f, respectively, and Γ_H is the total width of the Higgs boson.
- Only modifications of coupling strengths are considered, while the tensor structure of the Lagrangian is assumed to be the same as that in the SM. This assumes in particular that the observed state is a CP-even scalar, which can be tested using the measurements discussed in Ref. [30].

The coupling scale factors κ_j are defined in such a way that the cross sections σ_j and the partial decay widths Γ_j associated with the SM particle j scale with κ_j^2 compared to the SM prediction [10]. With this notation, and with κ_H^2 being the scale factor for the total Higgs boson width Γ_H, the signal strength for the $gg \to H \to \gamma\gamma$ process, for example, can be expressed as:

$$\frac{\sigma \cdot B\,(gg \to H \to \gamma\gamma)}{\sigma_{\mathrm{SM}}(gg \to H) \cdot B_{\mathrm{SM}}(H \to \gamma\gamma)} = \frac{\kappa_g^2 \cdot \kappa_\gamma^2}{\kappa_H^2} \tag{2}$$

In some of the fits, κ_H and the effective scale factors κ_γ, $\kappa_{(Z\gamma)}$, and κ_g for the loop-induced $H \to \gamma\gamma$, $H \to Z\gamma$, and $gg \to H$ processes are expressed as a function of the more fundamental factors κ_W, κ_Z, κ_t, κ_b, κ_τ, and κ_μ. Only the dominant fermion contributions are indicated here for simplicity, but other terms are included as well. The relevant relationships are:

$$\begin{aligned}
\kappa_g^2(\kappa_b, \kappa_t) &= \frac{\kappa_t^2 \cdot \sigma_{ggH}^{tt} + \kappa_b^2 \cdot \sigma_{ggH}^{bb} + \kappa_t\kappa_b \cdot \sigma_{ggH}^{tb}}{\sigma_{ggH}^{tt} + \sigma_{ggH}^{bb} + \sigma_{ggH}^{tb}} \\
\kappa_\gamma^2(\kappa_b, \kappa_t, \kappa_\tau, \kappa_W) &= \frac{\sum_{i,j} \kappa_i\kappa_j \cdot \Gamma_{\gamma\gamma}^{ij}}{\sum_{i,j} \Gamma_{\gamma\gamma}^{ij}} \\
\kappa_{(Z\gamma)}^2(\kappa_b, \kappa_t, \kappa_\tau, \kappa_W) &= \frac{\sum_{i,j} \kappa_i\kappa_j \cdot \Gamma_{Z\gamma}^{ij}}{\sum_{i,j} \Gamma_{Z\gamma}^{ij}} \\
\kappa_H^2 &= \sum_{\substack{jj=WW,\,ZZ,\,b\bar{b},\,\tau^-\tau^+,\\ \gamma\gamma,\,Z\gamma,\,gg,\,t\bar{t},\,c\bar{c},\,s\bar{s},\,\mu^-\mu^+}} \frac{\kappa_j^2 \Gamma_{jj}^{\mathrm{SM}}}{\Gamma_H^{\mathrm{SM}}}
\end{aligned} \tag{3}$$

where σ_{ggH}^{ij}, $\Gamma_{\gamma\gamma}^{ij}$, $\Gamma_{Z\gamma}^{ij}$ and $\Gamma_{ff}^{\mathrm{SM}}$ are theoretically predicted [10]. Unless dedicated fit parameters κ_γ, $\kappa_{(Z\gamma)}$, or κ_g are assigned to these effective coupling scale factors, the relations above are used in the fits.

3.2 Coupling fit results

The Higgs boson coupling scale factors are determined from a combined fit to all channels reported in Table 1, where the product $\sigma \cdot B\,(i \to H \to f)$ of cross section and branching ratio for all contributing Higgs signal channels is expressed as function of the coupling scale factors κ_i. Depending on the assumptions involved, different benchmark parametrizations are used following the recommendations in Ref. [10]. The benchmark parametrizations fall into two overall categories depending on assumptions on the total width. Some parametrizations make no assumptions on the total width, allowing only measurements of ratios $\lambda_{ij} = \kappa_i/\kappa_j$ of coupling scale factors. Others do make some assumptions, allowing absolute couplings κ_i to be extracted.

A detailed discussion of the treatment of the total width can be found in Ref. [10]. The total width is expected to be further constrained through measurements of the off-shell Higgs boson couplings [20], but these are unlikely to be sufficiently precise to replace such assumptions. Even in the absence of new decay modes, the Higgs total width can still differ from the SM expectation if any of its couplings to SM particles differ from their expected values.

The precision on a given coupling parameter is specific to the particular parametrization in which it is probed; general parametrizations with more parameters and fewer simplifying assumptions generally result in the parameters being determined with larger uncertainties.

A minimal coupling fit is shown in the parametrization with one universal coupling to vector bosons, $\kappa_V = \kappa_Z = \kappa_W$, and one universal coupling to fermions, $\kappa_F = \kappa_t = \kappa_b = \kappa_\tau = \kappa_\mu$. Such a measurement is most sensitive to different deviations from the SM between the Higgs boson gauge- and Yukawa-coupling sectors. In this parametrization, the $H \to \gamma\gamma$ and $gg \to H$ loops and the total Higgs boson width depend only on κ_F and κ_V, with no contributions from BSM physics. Experimental precisions of ~1.7% on κ_V and ~3.2% on κ_F are expected with 3000 fb^{-1} (~3.3% and ~5.1% with current theory uncertainties). This is a significant reduction compared to the 300 fb^{-1} expectations, which are ~2.5% on κ_V and ~7.1% on κ_F (~4.3% and ~8.8% with current theory uncertainties). The results are shown in Fig. 2 and in model Nr. 2 in Table 3.

Some extensions of this minimal coupling fit, which all assume no BSM Higgs decay modes, are shown in models Nr. 3–8 in Table 3. In model Nr. 3, the assumption on identical scaling between the W and Z bosons is removed to probe custodial symmetry. In model Nr. 4, a common scaling for vector bosons is kept but with separate couplings to up-type and down-type fermions. Similarly model Nr. 5 has separate couplings to quarks and leptons. Model Nr. 6 has separate couplings to quarks, the τ lepton, and the muon in order to probe differences between second and third-generation fermion couplings. In model Nr. 7 the assumption on identical scaling between the different gauge and Yukawa couplings is removed, while the assumption on no BSM particles contributing to the loops is kept. Finally, in model Nr. 8 the assumption on BSM particles in loops is removed in order to allow contributions from new physics, which results in a fit also including the effective coupling scale factors κ_g, κ_γ, and $\kappa_{(Z\gamma)}$. In general in these extended models the couplings to W and Z, as well as the loop-induced couplings to photons and gluons, are expected to be measured with ~4–5% experimental precision assuming 3000 fb^{-1}, while the fermion couplings have precisions of ~7–10%. Compared to the expectation for 300 fb^{-1} this is an improvement of up to a factor of 2, but with the statistically-limited precision on the muon coupling improving by the expected factor of ~3. The measurement precision for the $Z\gamma$ coupling improves by a factor of 1.5, being partially limited by experimental systematics with 3000 fb^{-1}.

Table 4 describes the expected precision for a coupling parametrization to probe loop-induced Higgs couplings κ_g, κ_γ, and $\kappa_{Z\gamma}$ and invisible or undetectable Higgs decays through their branching ratio $\mathrm{BR}_{i,u}$. All other couplings to massive particles that do not proceed via a loop in lowest order are assumed to be equal to their SM values. Within this model, this assumption which allows to probe $\mathrm{BR}_{i,u}$. A 95% CL upper limit of 10% on $\mathrm{BR}_{i,u}$ is attainable with 3000 fb^{-1} when including only experimental uncertainties, and 14% when current theory uncertainties are taken into account. Compared to the expectation for

Nr.	Coupling	300 fb^{-1} Theory unc.:			3000 fb^{-1} Theory unc.:		
		All	Half	None	All	Half	None
1	κ	4.2%	3.0%	2.4%	3.2%	2.2%	1.7%
2	$\boldsymbol{\kappa_V = \kappa_Z = \kappa_W}$	4.3%	3.0%	2.5%	3.3%	2.2%	1.7%
	$\boldsymbol{\kappa_F = \kappa_t = \kappa_b = \kappa_\tau = \kappa_\mu}$	8.8%	7.5%	7.1%	5.1%	3.8%	3.2%
3	κ_Z	4.7%	3.7%	3.3%	3.3%	2.3%	1.9%
	κ_W	4.9%	3.6%	3.1%	3.6%	2.4%	1.8%
	κ_F	9.3%	7.9%	7.3%	5.4%	4.0%	3.4%
4	κ_V	5.9%	5.4%	5.3%	3.7%	3.2%	3.0%
	κ_u	8.9%	7.7%	7.2%	5.4%	4.0%	3.4%
	κ_d	12%	12%	12%	6.7%	6.2%	6.1%
5	κ_V	4.3%	3.1%	2.5%	3.3%	2.2%	1.7%
	κ_q	11%	8.7%	7.8%	6.6%	4.5%	3.6%
	κ_l	10%	9.6%	9.3%	6.0%	5.3%	5.1%
6	κ_V	4.3%	3.1%	2.5%	3.3%	2.2%	1.7%
	κ_q	11%	9.0%	8.1%	6.7%	4.7%	3.8%
	κ_τ	12%	11%	11%	9.2%	8.4%	8.1%
	κ_μ	20%	20%	19%	6.9%	6.3%	6.1%
7	κ_Z	8.1%	7.9%	7.8%	4.3%	3.9%	3.8%
	κ_W	8.5%	8.2%	8.1%	4.8%	4.1%	3.9%
	κ_t	14%	12%	11%	8.2%	6.1%	5.3%
	κ_b	23%	22%	22%	12%	11%	10%
	κ_τ	14%	13%	13%	9.8%	9.0%	8.7%
	κ_μ	21%	21%	21%	7.3%	7.1%	7.0%
8	κ_Z	8.1%	7.9%	7.9%	4.4%	4.0%	3.8%
	κ_W	9.0%	8.7%	8.6%	5.1%	4.5%	4.2%
	κ_t	22%	21%	20%	11%	8.5%	7.6%
	κ_b	23%	22%	22%	12%	11%	10%
	κ_τ	14%	14%	13%	9.7%	9.0%	8.8%
	κ_μ	21%	21%	21%	7.5%	7.2%	7.1%
	κ_g	14%	12%	11%	9.1%	6.5%	5.3%
	κ_γ	9.3%	9.0%	8.9%	4.9%	4.3%	4.1%
	$\kappa_{Z\gamma}$	24%	24%	24%	14%	14%	14%

Table 3: Expected precision on Higgs coupling scale factors with 300 or 3000 fb^{-1} of $\sqrt{s}$ = 14 TeV data for selected parametrizations, assuming no decay modes beyond those in the SM. With SM decay modes only, the Higgs total width can still differ from the SM value if any of its couplings to SM particles differ from the expected values. The coupling scale factor $\boldsymbol{\kappa}$ represents all SM particles, $\boldsymbol{\kappa_V}$ represents the gauge bosons W and Z, $\boldsymbol{\kappa_F}$ represents all fermions, $\boldsymbol{\kappa_u}$ represents all up-type fermions, $\boldsymbol{\kappa_d}$ represents all down-type fermions, $\boldsymbol{\kappa_q}$ represents all quarks, and $\boldsymbol{\kappa_l}$ represents all leptons. The results are reported for 3 different assumptions on the theory uncertainties: the current size, half of the current size, and no theory uncertainties.

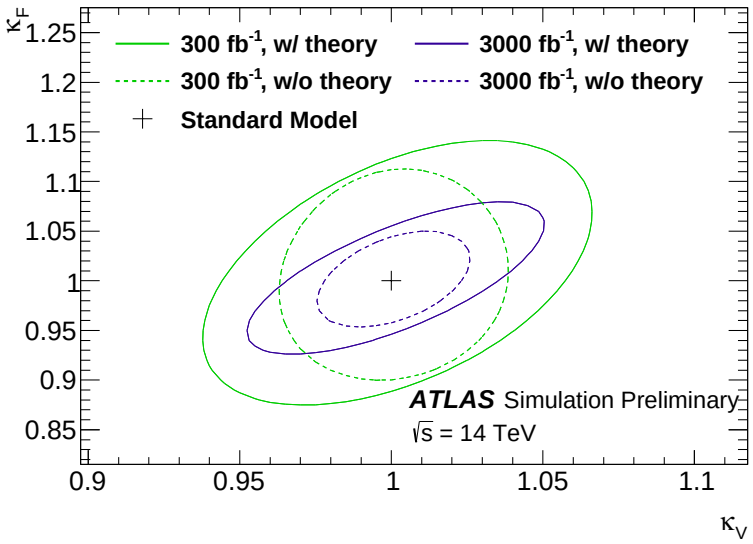

Figure 2: 68% CL expected likelihood contours for κ_V and κ_F in a minimal coupling fit at 14 TeV for an assumed integrated luminosity of 300 fb^{-1}and 3000 fb^{-1}.

300 fb^{-1} this is an improvement of up to a factor of 2.

When the assumption on the total width is removed and no other assumption is made, only ratios of coupling scale factors can be determined at the LHC. In this case $\sigma \cdot B\,(i \to H \to f)$ for all signal channels is a function of products of ratios $\lambda_{XY} = \kappa_X/\kappa_Y$ of coupling scale factors giving the proportionality $\sigma \cdot B\,(i \to H \to f) \sim \lambda_{iY}^2 \cdot \kappa_{YY'}^2 \cdot \lambda_{fY}^2$, where $\kappa_{YY'} = \kappa_Y \cdot \kappa_{Y'}/\kappa_H$ is a suitable chosen overall scale parameter common to all signal channels and λ_{iY} and λ_{fY} are the coupling scale factor ratios involving the initial and final state particles, respectively. In addition to avoiding the assumption on the total width, ratios of coupling scale factors also have the advantage that many experimental and theoretical systematic uncertainties cancel (such as the uncertainty on the integrated luminosity).

The expected precision on ratios of coupling parameters is given in Table 5 for selected bechmark parametrizations. The first five benchmarks are targeted at specific aspects of the SM: benchmark model Nr. 10 for the ratio of fermion and gauge boson couplings, Nr. 11 for the ratio of W and Z couplings, Nr. 12 for the ratio of down- and up-type fermion couplings, and Nr. 13 for the ratio of lepton and

Nr.	Parameter	300 fb^{-1} Theory unc.:			3000 fb^{-1} Theory unc.:		
		All	Half	None	All	Half	None
9	κ_g	8.9%	7.1%	6.3%	6.7%	4.1%	2.8%
	κ_γ	4.9%	4.8%	4.7%	2.1%	1.8%	1.7%
	$\kappa_{Z\gamma}$	23%	23%	23%	14%	14%	14%
	BR$_{i,u}$	<22%	<20%	<20%	<14%	<11%	<10%

Table 4: Expected precision on the loop-induced Higgs couplings κ_g, κ_γ, and $\kappa_{Z\gamma}$, along with the expected 95% CL upper limit on the branching ratio for invisible or undetectable Higgs decays, BR$_{i,u}$, with 300 and 3000 fb^{-1} at $\sqrt{s}$ = 14 TeV. Other couplings to massive particles are assumed to be equal to their SM values, but no other assumptions are made relating to the Higgs total width.

quark couplings, and Nr. 14 for the ratio of second- and third-generation lepton couplings. At 3000 fb^{-1} experimental uncertainties between ~1.5% and ~10% are possible for these ratios, which will test the SM to a high degree of precision. In many cases an improvement of a factor of 2 compared to the expectation for 300 fb^{-1} is obtained, as some experimental systematic uncertainties do not scale down with the luminosity increase. When the current theory uncertainties are taken into account, these precisions on the ratios are only slightly degraded.

A fully generic benchmark parametrization is also used that does not need any assumptions beyond those in Sec. 3.1 and making no assumption on new particles contributing through loops. The experimental precision on the ratios of coupling scale factors is summarized in Fig. 3 and in model Nr. 15 in Table 5. For the majority of these coupling ratios, the precision without theory uncertainties is significantly improved by more than a factor of 2 with 3000 fb^{-1} compared to 300 fb^{-1}. For 3000 fb^{-1} the precision ranges from ~2% for the best-determined coupling scale factor ratio between the electroweak bosons to ~5–8% for the ratios involving gluons and the second- and third-generation fermions (~3-10% including current theory uncertainties). The coupling ratio involving the very small loop-induced $Z\gamma$ coupling is determined at the 14% level with 3000 fb^{-1}.

The ratio of the photon and Z boson couplings, $\lambda_{\gamma Z}$, is particularly important to look for indications of new charged particles contributing in the $H \to \gamma\gamma$ loop in comparison to $H \to ZZ$ decays. The experimental precision on $\lambda_{\gamma Z}$ will improve by about a factor of 3 from 5.1% with 300 fb^{-1} to 1.8% with 3000 fb^{-1}; with theory uncertainties, an improvement of a factor of about 2 is attained. The ratio of the top quark and gluon couplings, λ_{tg}, is similarly crucial for possible new colored particles contributing through the gluon fusion loop as compared to ttH. Without theory uncertainties, it will be measured to 15% precision with 300 fb^{-1} and improves by a factor of 3 to 5.0% with 3000 fb^{-1}. The improvement is a factor of ~1.5 with theory uncertainties.

Differential measurements of Higgs production, for example of the Higgs boson transverse momentum and rapidity [31,32], are not included here and will further decrease the uncertainties in the coupling measurements. The ttH process is expected to be measured in additional decay channels to those studied here. These and other improvements are expected to further improve the Higgs coupling precision attained in the future.

Nr.	Coupling ratio	300 fb^{-1} Theory unc.:			3000 fb^{-1} Theory unc.:		
		All	Half	None	All	Half	None
10	κ_{VV}	7.3%	6.7%	6.5%	4.0%	3.2%	2.9%
	λ_{FV}	7.8%	7.4%	7.2%	3.6%	3.1%	2.9%
11	κ_{ZZ}	9.8%	9.1%	8.9%	5.1%	4.3%	3.9%
	λ_{WZ}	4.3%	4.0%	3.9%	2.3%	1.8%	1.6%
	λ_{FZ}	9.2%	8.5%	8.3%	4.4%	3.7%	3.5%
12	κ_{uu}	14%	11%	9.7%	8.7%	5.7%	4.2%
	λ_{Vu}	9.4%	8.3%	7.9%	5.1%	3.8%	3.2%
	λ_{du}	9.7%	8.2%	7.7%	6.0%	4.6%	4.0%
13	κ_{qq}	14%	11%	9.9%	8.1%	5.6%	4.5%
	λ_{Vq}	9.6%	8.5%	8.1%	5.2%	3.9%	3.4%
	λ_{lq}	12%	10%	9.4%	7.3%	6.0%	5.4%
14	$\kappa_{\tau\tau}$	21%	19%	19%	17%	15%	15%
	$\lambda_{V\tau}$	11%	11%	11%	8.5%	7.8%	7.6%
	$\lambda_{q\tau}$	12%	10%	9.8%	9.3%	7.9%	7.4%
	$\lambda_{\mu\tau}$	22%	22%	22%	11%	9.8%	9.6%
15	κ_{gZ}	6.4%	4.4%	3.5%	5.7%	3.3%	2.0%
	λ_{WZ}	5.2%	4.8%	4.6%	3.1%	2.4%	2.1%
	λ_{tg}	17%	16%	15%	9.4%	6.4%	5.0%
	λ_{bZ}	18%	17%	17%	9.8%	8.1%	7.4%
	$\lambda_{\tau Z}$	12%	12%	11%	8.9%	8.1%	7.8%
	$\lambda_{\mu Z}$	20%	20%	20%	6.3%	6.2%	6.1%
	λ_{gZ}	13%	11%	10%	8.7%	5.8%	4.5%
	$\lambda_{\gamma Z}$	5.5%	5.2%	5.1%	2.6%	2.0%	1.8%
	$\lambda_{(Z\gamma)Z}$	23%	23%	23%	14%	14%	14%
16	$\kappa_{\gamma\gamma}$	14%	13%	12%	6.8%	5.5%	5.0%
	$\lambda_{Z\gamma}$	5.5%	5.2%	5.1%	2.5%	2.0%	1.8%
	$\lambda_{W\gamma}$	5.9%	5.7%	5.6%	2.7%	2.4%	2.2%
	$\lambda_{t\gamma}$	21%	20%	20%	10%	8.0%	7.0%
	$\lambda_{b\gamma}$	18%	17%	17%	9.5%	8.0%	7.4%
	$\lambda_{\tau\gamma}$	13%	12%	12%	8.7%	8.1%	7.9%
	$\lambda_{\mu\gamma}$	20%	20%	20%	6.5%	6.2%	6.1%
	$\lambda_{g\gamma}$	13%	12%	11%	8.5%	5.9%	4.6%
	$\lambda_{(Z\gamma)\gamma}$	23%	23%	23%	14%	14%	14%

Table 5: Expected precision on ratios of Higgs coupling scale factors with 300 or 3000 fb^{-1} of $\sqrt{s}$ = 14 TeV data, for selected benchmark parametrizations without assumptions on the Higgs total width. The results are reported for 3 different assumption on theory uncertainties: the current size, half of the current size and no theory uncertainties.

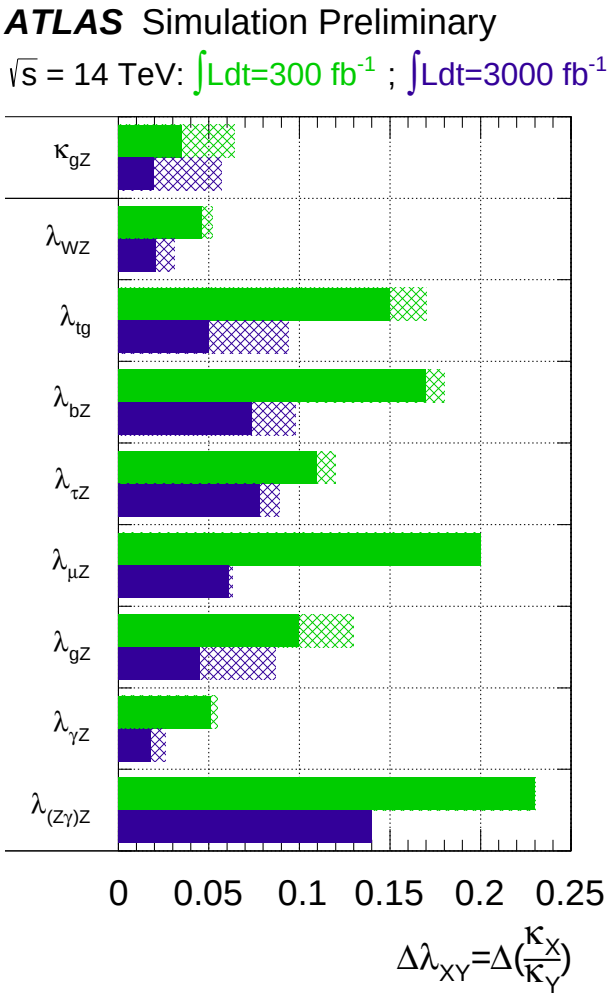

Figure 3: Relative uncertainty expected for the determination of coupling scale factor ratios λ_{XY} in a generic fit without assumptions, assuming a SM Higgs boson with a mass of 125 GeV and with 300 fb^{-1} or 3000 fb^{-1} of 14 TeV LHC data. The hashed areas indicate the increase of the estimated error due to current theory systematic uncertainties. The numerical values can be found in model Nr. 15 in Table 5.

3.3 Mass dependence of couplings

To test the predicted relationship between the Higgs boson couplings and the SM particle masses, "reduced" coupling scale factors y_i are defined[2] as in Eqns. (16) and (18) in Ref. [33]:

$$y_{V,i} = \sqrt{\kappa_{V,i}\frac{g_{V,i}}{2v}} = \sqrt{\kappa_{V,i}}\frac{m_{V,i}}{v} \quad (4)$$

for the weak bosons V=W and Z (indexed by i), and

$$y_{F,i} = \kappa_{F,i}\frac{g_{F,i}}{\sqrt{2}} = \kappa_{F,i}\frac{m_{F,i}}{v} \quad (5)$$

for the fermions F=μ, τ, b, and t (indexed by i), and where $g_{V,i}$ and $g_{F,i}$ denote the absolute gauge couplings to various bosons and Yukawa couplings to various fermions, respectively. The fit results for a model assuming no new Higgs decay modes, with loop-induced couplings resolved in terms of the couplings to particles running in the loops (see Table 3, model Nr. 7), are used. Figure 4 shows the reduced coupling scale factors y_i as a function of the mass of particle i.

3.4 Theory uncertainties

As seen from the expected precision of coupling parameter measurements in Tables 3–5, the current Higgs boson signal theory uncertainties [10–12] give a sizeable contribution to the expected total uncertainty and even dominate the uncertainty in some cases. This section provides estimates of how much each source of theory uncertainty would have to be reduced to be small compared to the expected experimental uncertainties. In this context "small" is arbitrarily defined for each theory systematic uncertainty as 30% of the expected total experimental uncertainty, which would lead to an increase of the total uncertainty by ~10% due to this source[3].

This estimation of the size of theory uncertainties is only approximate and is intended as a guideline to indicate where improvements are definitely needed, rather than as a precise prediction. In some cases such as the jet-bin and p_T uncertainties for the $gg \to H$ process, the values of the uncertainties are specific to the analysis selection, but are treated as 100% correlated between the different analyses since this is the best approximation currently possible. However, this allows the high-statistics fits in the HL-LHC scenarios to reduce the input theory uncertainty by up to a factor of 2 by exploiting the consistency of the signal strength between different experimental analyses, categories, and bins in distributions. These reduction factors are overstated as they originate from an insufficiently detailed model of the underlying theory uncertainties and their correlatations in different phase space regions. More detailed correlation models and improved analysis, which allow for better cancellation of systematic uncertainties in some measurements, will need to be developed in the future either to address this issue or to demonstrate where measured data can be used to reduce the Higgs boson signal theory uncertainties. The deduced theory uncertainties given here are corrected as best as possible to compensate for these excessive reductions in uncertainty.

Table 6 shows the deduced sizes of different Higgs boson signal theoretical uncertainties given the measurements presented in the generic model 15 in Table 5, which uses as few theory assumptions as possible at the LHC. Models 2 and 8 from Table 3 were also examined, but no stronger constraints were found.

In general, both the inclusive and differential signal theory uncertainties on the $gg \to H$ process are found to be the most limiting for future measurements. To a lesser degree, the uncertainties on the

[2]The definition of the reduced vector boson coupling, $y_{V,i}$, has been changed with respect to the one used in Ref. [4].

[3]As the theory uncertainties are uncorrelated to the experimental uncertainties, a sum in quadrature with the experimental uncertainties is valid to very good approximation.

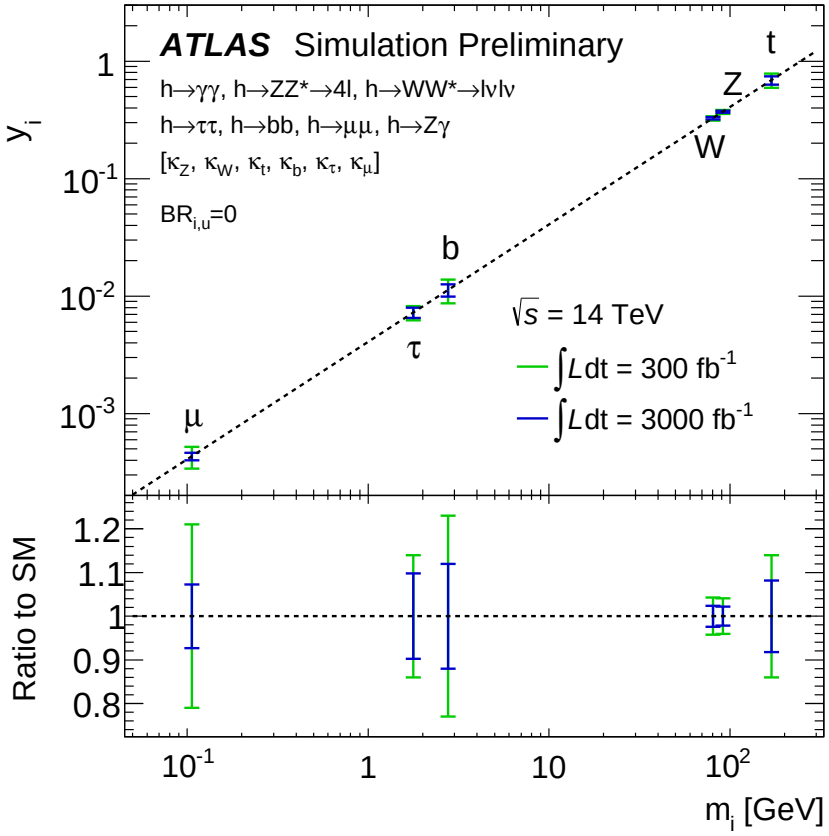

Figure 4: Fit results for the reduced coupling scale factors $y_{V,i} = \sqrt{\kappa_{V,i}\frac{g_{V,i}}{2v}} = \sqrt{\kappa_{V,i}}\frac{m_{V,i}}{v}$ for weak bosons and $y_{F,i} = \kappa_{F,i}\frac{g_{F,i}}{\sqrt{2}} = \kappa_{F,i}\frac{m_{F,i}}{v}$ for fermions as a function of the particle mass, assuming 300 fb^{-1} or 3000 fb^{-1} of 14 TeV data and a SM Higgs boson with a mass of 125 GeV. The corresponding uncertainties on the coupling scale factors can be found in model Nr. 7 in Table 3. The diagonal, dashed line indicates the predicted mass dependence for the SM Higgs boson.

Scenario	Status 2014	Deduced size of uncertainty to increase total uncertainty by $\lesssim$10% for 300 fb^{-1}			by $\lesssim$10% for 3000 fb^{-1}				
Theory uncertainty (%)	[10–12]	κ_{gZ}	λ_{gZ}	$\lambda_{\gamma Z}$	κ_{gZ}	$\lambda_{\gamma Z}$	λ_{gZ}	$\lambda_{\tau Z}$	λ_{tg}
$gg \to H$									
PDF	8	2	-	-	1.3	-	-	-	-
incl. QCD scale (MHOU)	7	2	-	-	1.1	-	-	-	-
p_T shape and 0j $\to$ 1j mig.	10–20	-	3.5–7	-	-	1.5–3	-	-	-
1j $\to$ 2j mig.	13–28	-	-	6.5–14	-	3.3–7	-	-	-
1j $\to$ VBF 2j mig.	18–58	-	-	-	-	-	6–19	-	-
VBF 2j $\to$ VBF 3j mig.	12–38	-	-	-	-	-	-	6–19	-
VBF									
PDF	3.3	-	-	-	-	-	2.8	-	-
$t\bar{t}H$									
PDF	9	-	-	-	-	-	-	-	3
incl. QCD scale (MHOU)	8	-	-	-	-	-	-	-	2

Table 6: Estimation of the deduced size of theory uncertainties, in percent (%), for different Higgs coupling measurements in the generic Model 15 from Table 5, requiring that each source of theory systematic uncertainty affects the measurement by less than 30% of the total experimental uncertainty and hence increase the total uncertainty by less than 10%. A dash "-" indicates that the theory uncertainty from existing calculations [10–12] is already sufficiently small to fulfill the condition above for some measurements. The same applies to theory uncertainties not mentioned in the table for any measurement. The impact of the jet-bin and p_T related uncertainties in $gg \to H$ depends on analysis selections and hence no single number can be quoted. Therefore the range of uncertainty values used in the different analysis is shown.

$t\bar{t}H$ and VBF production also contribute. Other uncertainties, such as the parametric m_b or $H \to \gamma\gamma$ and $H \to Z\gamma$ theory uncertainties entering the branching ratio calculation, increase the total uncertainty on the measurements by only 5–10% and are hence already below the goal of an increase by 10%. Therefore they are not explicitly mentioned in Table 6. However, there are several of these smaller sources so improved calculations in these areas will help to improve the ultimate precision of future LHC Higgs measurements.

In some cases where the experimental uncertainty is very small, such as $\kappa_{gZ} = \kappa_g \cdot \kappa_Z / \kappa_H$, the inclusive missing higher order uncertainty (MHOU) on $gg \to H$, estimated from QCD scale variations, would need to be reduced by up to a factor of ~6 in order to increase the total uncertainty by less than the goal of ~10%. Such a reduction seems very ambitious so this uncertainty may remain significant for Higgs measurements at the HL-LHC.

Finally, it should be noted that the κ-framework is itself an approximation as discussed in the beginning of Sec. 3. Currently there are no theory uncertainties assigned for these approximations, although they could become significant at the HL-LHC.

4 Conclusions

Several new Higgs boson production and decay modes can be observed by the ATLAS detector with 3000 fb^{-1} at the HL-LHC compared to a sample of 300 fb^{-1} that will be accumulated before the Phase-II upgrades, and the precision of all channels can be improved. Compared to previous studies, analyses in the $H \to Z\gamma$ and $VH/ttH \to \gamma\gamma$ channels have been refined, and the $VH \to b\bar{b}$ channel has now been

explored. The projected measurements of cross section times branching ratio using the combination of all channels studied are used to derive the expected precision on Higgs boson couplings to fermions and bosons, and on the ratios of couplings, in a variety of parametrizations. The expected limit on the Higgs inviisible branching ratio is also determined. With 3000 fb^{-1} of data, in many cases the expected precision is improved by a significant amount compared to 300 fb^{-1}. The improvements at high luminosity are as large as a factor of 2–3, particularly without the inclusion of theoretical systematic uncertainties which are expected to be improved in the future.

References

[1] ATLAS Collaboration, *Physics at a High-Luminosity LHC with ATLAS (Update)*, ATL-PHYS-PUB-2012-004 (2012). https://cdsweb.cern.ch/record/1484890.

[2] R. Aleksan et al., *Physics Briefng Book, Input for the Strategy Group to draft the update of the European Strategy for Particle Physics*, CERN-ESG-005 (2013). http://europeanstrategygroup.web.cern.ch/europeanstrategygroup/Briefing_book.pdf.

[3] ATLAS Collaboration, *Letter of Intent for the Phase-II Upgrade of the ATLAS Experiment*, CERN-LHCC-2012-022 (2012). https://cds.cern.ch/record/1502664.

[4] ATLAS Collaboration, *Projections for measurements of Higgs boson cross sections, branching ratios and coupling parameters with the ATLAS detector at a HL-LHC*, ATL-PHYS-PUB-2013-014 (2013). https://cds.cern.ch/record/1611186.

[5] ATLAS Collaboration, *Performance assumptions for an upgraded ATLAS detector at a High-Luminosity LHC*, ATL-PHYS-PUB-2013-004 (2013). https://cds.cern.ch/record/1527529.

[6] ATLAS Collaboration, *Performance assumptions based on full simulation for an upgraded ATLAS detector at a High-Luminosity LHC*, ATL-PHYS-PUB-2013-009 (2013). https://cds.cern.ch/record/1604420.

[7] ATLAS Collaboration, *Update of the prospects for the $H \to Z\gamma$ search at the High-Luminosity LHC*, ATL-PHYS-PUB-2014-006 (2014). https://cds.cern.ch/record/1703276.

[8] ATLAS Collaboration, *HL-LHC projections for signal and background yield measurements of the $H \to \gamma\gamma$ when the Higgs boson is produced in association with t quarks, W or Z bosons*, ATL-PHYS-PUB-2014-012 (2014). https://cds.cern.ch/record/1741011.

[9] ATLAS Collaboration, *Prospects for the study of the Higgs boson in the VH(bb) channel at HL-LHC*, ATL-PHYS-PUB-2014-011 (2014). https://cds.cern.ch/record/1740962.

[10] LHC Higgs Cross Section Working Group, *Handbook of LHC Higgs Cross Sections: 3. Higgs Properties*, arXiv:1307.1347 [hep-ph].

[11] LHC Higgs Cross Section Working Group. https://twiki.cern.ch/twiki/bin/view/LHCPhysics/CrossSections.

[12] Higgs cross sections for European Strategy studies in 2012 . https://twiki.cern.ch/twiki/bin/view/LHCPhysics/HiggsEuropeanStrategy2012.

[13] ATLAS Collaboration, *Studies of the VBF $H \to \tau_l\tau_{\text{had}}$ Analysis at High-Luminosity LHC Conditions*, ATL-PHYS-PUB-2014-018 (2014). http://atlas.web.cern.ch/Atlas/GROUPS/PHYSICS/PUBNOTES/ATL-PHYS-PUB-2014-018.

[14] C. Englert, M. McCullough, and M. Spannowsky, *Gluon-initiated associated production boosts Higgs physics*, Phys. Rev. **D89** no. 1, (2014) 013013, arXiv:1310.4828 [hep-ph].

[15] ATLAS Collaboration, *Search for Invisible Decays of a Higgs Boson Produced in Association with a Z Boson in ATLAS*, Phys. Rev. Lett. **112** (2014) 201802, arXiv:1402.3244 [hep-ex].

[16] N. Kauer and G. Passarino, *Inadequacy of zero-width approximation for a light Higgs boson signal*, arXiv:1206.4803 [hep-ph].

[17] F. Caola and K. Melnikov, *Constraining the Higgs boson width with ZZ production at the LHC*, Phys. Rev. **D 88** (2013) 054024, arXiv:1307.4935 [hep-ph].

[18] J. M. Campbell, R. K. Ellis, and C. Williams, *Bounding the Higgs width at the LHC using full analytic results for $gg \to e^-e^+\mu^-\mu^+$*, JHEP **04** (2014) 060, arXiv:1311.3589 [hep-ph].

[19] J. M. Campbell, R. K. Ellis, and C. Williams, *Bounding the Higgs width at the LHC: complementary results from $H \to WW$*, Phys.Rev. **D 89** (2014) 053011, arXiv:1312.1628 [hep-ph].

[20] ATLAS Collaboration, *Determination of the off-shell Higgs boson signal strength in the high-mass ZZ final state with the ATLAS detector*, ATLAS-CONF-2014-042 (2014). https://cds.cern.ch/record/1740973.

[21] ATLAS Collaboration, *Measurements of Higgs boson production and couplings in diboson final states with the ATLAS detector at the LHC*, Phys. Lett. **B 726** (2013) 88, arXiv:1307.1427 [hep-ex].

[22] ATLAS Collaboration, *Combined search for the Standard Model Higgs boson in pp collisions at $\sqrt{s}$=7 TeV with the ATLAS detector*, Phys. Rev. **D 86** (2012) 032003, arXiv:1207.0319 [hep-ex].

[23] ATLAS and CMS Collaborations, *Procedure for the LHC Higgs boson search combination in Summer 2011*, ATL-PHYS-PUB-2011-011, CERN-CMS-NOTE-2011-005 (2011). http://cdsweb.cern.ch/record/1375842.

[24] L. Moneta et al., *The RooStats Project*, PoS **ACAT2010** (2010) 057, arXiv:1009.1003 [physics.data-an].

[25] K. Cranmer et al., *HistFactory: A tool for creating statistical models for use with RooFit and RooStats*, CERN-OPEN-2012-016 (2012). http://cdsweb.cern.ch/record/1456844.

[26] W. Verkerke *et al.*, "The roofit toolkit for data modelling." Available from http://roofit.sourceforge.net or with recent versions of the root framework available at http://root.cern.ch.

[27] ATLAS Collaboration, *Observation and measurement of Higgs boson decays to WW^* with ATLAS at the LHC*, ATLAS-CONF-2014-060 (2014). https://cds.cern.ch/record/1954714.

[28] ATLAS Collaboration, *Search for the $b\bar{b}$ decay of the Standard Model Higgs boson in associated $(W/Z)H$ production with the ATLAS detector*, arXiv:1409.6212 [hep-ex].

[29] ATLAS Collaboration, *Search for the Standard Model Higgs boson in $H \to \tau^+\tau^-$ decays in proton-proton collisions with the ATLAS detector*, ATLAS-CONF-2012-160 (2012). http://cds.cern.ch/record/1493624.

[30] ATLAS Collaboration, *Prospects for measurements of tensor structure of the HZZ vertex in $H \to ZZ^* \to 4l$ decay with ATLAS detector*, ATL-PHYS-PUB-2013-013 (2013). https://cds.cern.ch/record/1611123/.

[31] ATLAS Collaboration, *Measurements of fiducial and differential cross sections for Higgs boson production in the diphoton decay channel at $\sqrt{s} = 8$ TeV with ATLAS*, arXiv:1407.4222 [hep-ex].

[32] ATLAS Collaboration, *Fiducial and differential cross sections of Higgs boson production measured in the four-lepton decay channel in pp collisions at $\sqrt{s}$=8 TeV with the ATLAS detector*, arXiv:1408.3226 [hep-ex].

[33] M. Spira, R. Tanaka. https://twiki.cern.ch/twiki/bin/view/LHCPhysics/SMInputParameter#MSbar_running_masses_for_the_qua.

A Ratio of Higgs couplings vs. mass

To test the predicted relationship between the Higgs boson couplings and the SM particle masses, "reduced" coupling scale factors y_i have been defined in Sec. 3.3. In this appendix, the ratios of these reduced coupling scaled factors to the photon coupling are probed using the fit results for a fully generic model without assumptions (model Nr. 16 of Table 5). The fit parameters are ratios of couplings to κ_γ, with $\kappa_\gamma\kappa_\gamma/\kappa_H$ as the overall scale parameter. Hence the fitted coupling scale factor ratios are $\lambda_{\mu\gamma} = \kappa_\mu/\kappa_\gamma$, $\lambda_{\tau\gamma} = \kappa_\tau/\kappa_\gamma$, $\lambda_{t\gamma} = \kappa_t/\kappa_\gamma$, $\lambda_{W\gamma} = \kappa_W/\kappa_\gamma$, $\lambda_{Z\gamma} = \kappa_Z/\kappa_\gamma$, $\lambda_{g\gamma} = \kappa_g/\kappa_\gamma$, $\lambda_{(Z\gamma)\gamma} = \kappa_{(Z\gamma)}/\kappa_\gamma$, and $\kappa_{\gamma\gamma} = \kappa_\gamma\kappa_\gamma/\kappa_H$.

Figure 5 shows the ratios $y_{V,i}/\sqrt{\kappa_\gamma}$ for weak bosons and $y_{F,i}/\kappa_\gamma$ for fermions, calculated from the ratios $\lambda_{i\gamma} = \kappa_i/\kappa_\gamma$, as a function of the mass for particle i. For completeness, the uncertainty on the gluon-coupling ratio measurement κ_g/κ_γ, which can be used as an indirect measurement of the top-coupling through the $gg \to H$ process, is also shown next to the expected measurement for y_t/κ_γ which uses the direct ttH process. The uncertainty on the coupling ratio $\kappa_{(Z\gamma)}/\kappa_\gamma$ is not shown.

B Vector boson and fermion couplings

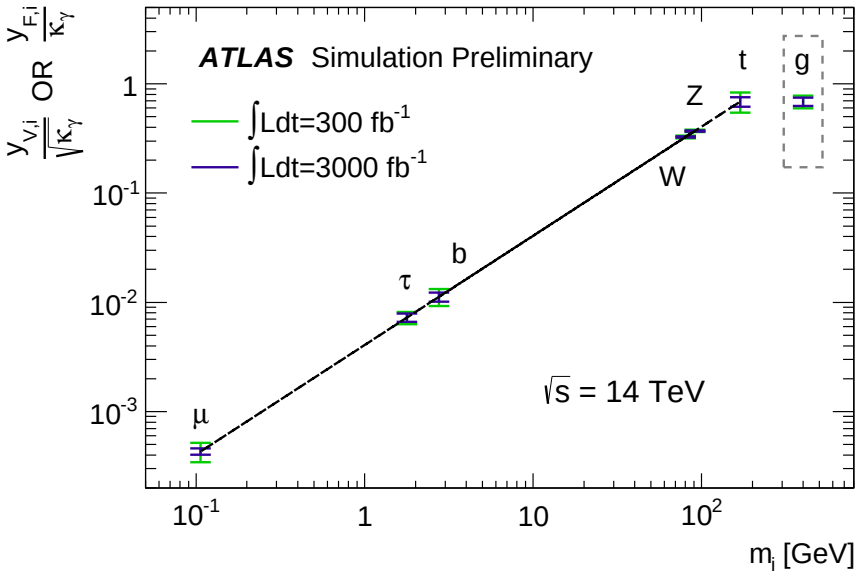

Figure 5: Fit results for ratios of reduced coupling scaled factors to the photon coupling, $y_{V,i}/\sqrt{\kappa_\gamma}$ for weak bosons and $y_{F,i}/\kappa_\gamma$ for fermions, as a function of the mass of particle i, assuming 300 fb^{-1} and 3000 fb^{-1} at 14 TeV and a SM Higgs boson with a mass of 125 GeV. For completeness, the uncertainty on the gluon-coupling ratio measurement κ_g/κ_γ, which can be used as an indirect measurement of the top-coupling through the $gg \rightarrow H$ process, is also shown next to the expected measurement for y_t/κ_γ which uses the direct ttH process. The uncertainty on the coupling ratio $\kappa_{(Z\gamma)}/\kappa_\gamma$ is not shown. The relative uncertainties on the corresponding ratios of couplings can be found in model Nr. 16 in Table 5. The diagonal, solid line indicates the predicted mass dependence for the SM Higgs boson.

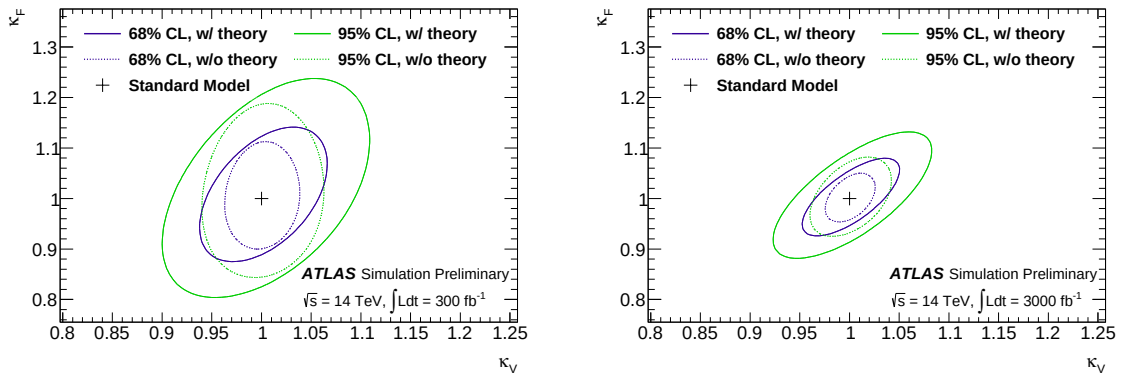

Figure 6: 68% and 95% CL expected likelihood contours for κ_V and κ_F in a minimal coupling fit at 14 TeV for an assumed integrated luminosity of 300 fb^{-1} (left) and for 3000 fb^{-1} (right).